J|A|C|S
ARTICLES
Published on Web 08/02/2002

The Active Site of Cellobiohydrolase Cel6A from *Trichoderma reesei*: The Roles of Aspartic Acids D221 and D175

Anu Koivula,[†] Laura Ruohonen,[†] Gerd Wohlfahrt,[†,#] Tapani Reinikainen,[†] Tuula T. Teeri,[*,†,+] Kathleen Piens,[‡] Marc Claeyssens,[‡] Martin Weber,[§] Andrea Vasella,[§] Dieter Becker,[||] Michael L. Sinnott,[*,||] Jin-yu Zou,[⊥] Gerard J. Kleywegt,[⊥] Michael Szardenings,[⊥,¥] Jerry Ståhlberg,[⊥] and T. Alwyn Jones[*,⊥]

Contribution from VTT Biotechnology, P.O. Box 1500, FIN-02044 VTT, Espoo, Finland, Laboratory of Biochemistry, State University of Ghent, K.L. Ledeganckstraat 35, B-9000 Ghent, Belgium, Laboratory for Organic Chemistry, Swiss Federal Institute of Technology, ETH-Zentrum, Universitätsstrasse 16, CH-8092 Switzerland, Department of Paper Science, UMIST, P.O. Box 88, Sackville Street, Manchester M60 1QD, England, and Department of Cell and Molecular Biology, Uppsala University, Biomedical Center Box 596, S-75124, Uppsala, Sweden

Received December 4, 2001

Abstract: *Trichoderma reesei* cellobiohydrolase Cel6A is an inverting glycosidase. Structural studies have established that the tunnel-shaped active site of Cel6A contains two aspartic acids, D221 and D175, that are close to the glycosidic oxygen of the scissile bond and at hydrogen-bonding distance from each other. Here, site-directed mutagenesis, X-ray crystallography, and enzyme kinetic studies have been used to confirm the role of residue D221 as the catalytic acid. D175 is shown to affect protonation of D221 and to contribute to the electrostatic stabilization of the partial positive charge in the transition state. Structural and modeling studies suggest that the single-displacement mechanism of Cel6A may not directly involve a catalytic base. The value of $^{D2O}(V)$ of 1.16 ± 0.14 for hydrolysis of cellotriose suggests that the large direct effect expected for proton transfer from the nucleophilic water through a water chain (Grotthus mechanism) is offset by an inverse effect arising from reversibly breaking the short, tight hydrogen bond between D221 and D175 before catalysis.

Introduction

Cellulose is an insoluble material composed of long chains of β-1,4 linked glucosyl units. Native cellulose can be completely degraded to soluble sugars by synergistic mixtures of many different types of cellulases produced by a wide range of microbes.[1,2] The soft rot fungus *Trichoderma reesei* produces an effective mixture of cellulases. The most abundant enzymes are two cellobiohydrolases, Cel7A and Cel6A, formerly called CBHI and CBHII,[3] and these are also the enzymes that are most efficient on highly crystalline cellulose. The two cellobiohydrolases have active sites enclosed in tunnels formed by long loops on the surface of the catalytic domains, and they therefore act primarily at the cellulose chain ends.[4−9] Cel7A removes cellobiose units from the reducing end, while Cel6A prefers the nonreducing end.[4,7−9] In keeping with their extended substrate-binding sites, Cel7A and Cel6A are processive enzymes catalyzing several bond cleavages before the dissociation of the enzyme−substrate complex.[2,4]

The reaction mechanisms for all cellulases appear to involve partial proton donation to the leaving group by a carboxylic acid group on the enzyme. Hydrolysis occurs with retention or inversion of the anomeric configuration depending on the nature of the nucleophile. If the nucleophile is a carboxylate group of the enzyme, then a double displacement mechanism occurs.[10]

* To whom correspondence should be addressed. T.T.T. (phone) +46-8-55378381, (fax) +46-8-55378483, (e-mail) Tuula@biochem.kth.se; M.L.S. (phone) +44-161-200-3897, (fax) +44-161-200-3858, (e-mail) michael.sinnott@umist.ac.uk; T.A.J. (phone) +46-18-4714982, (fax) +46-18-536971, (e-mail) alwyn@xray.bmc.uu.se.
[†] VTT Biotechnology.
[‡] State University of Ghent.
[§] Swiss Federal Institute of Technology.
[||] UMIST.
[⊥] Uppsala University.
[#] Present address: Orion Corp, P.O. Box 65, FIN-02101 Espoo, Finland.
[+] Present address: Department of Biotechnology, Royal Institute of Technology, SCFAB, S-10691 Stockholm, Sweden.
[¥] Present address: Cosmix Molecular Biologicals GMBH, Mascheroder Weg 1B, D-38124 Braunschweig, Germany.

(1) Wood, T. M.; Garcia-Campayo, V. *Biodegradation* **1990**, *1*, 147−161.
(2) Teeri, T. T. *Trends Biotechnol.* **1997**, *15*, 160−167.
(3) Henrissat, B.; Teeri, T. T.; Warren, R. A. *FEBS Lett.* **1998**, *425*, 352−4.
(4) Rouvinen, J.; Bergfors, T.; Teeri, T.; Knowles, J. K.; Jones, T. A. *Science* **1990**, *249*, 380−6.
(5) Srisodsuk, M.; Kleman-Leyer, K.; Keranen, S.; Kirk, T. K.; Teeri, T. T. *Eur. J. Biochem.* **1998**, *251*, 885−92.
(6) Kleman-Leyer, K.; Siika-aho, M.; Teeri, T. T.; Kirk, T. K. *Appl. Environ. Microbiol.* **1996**, *62*, 2883−2887.
(7) Divne, C.; Stahlberg, J.; Reinikainen, T.; Ruohonen, L.; Pettersson, G.; Knowles, J. K.; Teeri, T. T.; Jones, T. A. *Science* **1994**, *265*, 524−8.
(8) Divne, C.; Stahlberg, J.; Teeri, T. T.; Jones, T. A. *J. Mol. Biol.* **1998**, *275*, 309−25.
(9) Barr, B. K.; Wolfgang, D. E.; Piens, K.; Claeyssens, M.; Wilson, D. B. *Biochemistry* **1998**, *37*, 9220−9.

A covalent glycosyl-enzyme intermediate is formed and then hydrolyzed with the acid catalyst now acting as a general base for the deprotonation of an incoming water molecule. Cel7A is such a retaining glycosidase.[11,12] If, on the other hand, the nucleophile is a water molecule, a single displacement occurs, in which the water molecule is deprotonated by an enzyme carboxylate group, acting as a general base. Because a water molecule is placed between the reaction center and the enzyme carboxylate group of inverting enzymes, the two catalytic carboxyl and carboxylate groups tend to be further apart in inverting enzymes.[13] Cel6A and the other enzymes in family 6 are inverting glycosidases.[11,12]

The structure determination of the catalytic domains of both *T. reesei* cellobiohydrolases has paved the way for detailed studies of their catalytic machineries.[4,7,8,14−18] In Cel6A, the extended active site can accommodate six glucosyl units.[17,18] The binding of four glucosyl units within the tunnel, corresponding to the −2 to +2 sites, contributes to the transition-state stabilization,[4,19,20] while binding to the +4 site is apparently only required for the action of Cel6A on crystalline substrates.[15] The early structural studies of Cel6A revealed a network of interacting residues apparently contributing to the formation of the active site.[4] Two aspartic acids, D221 and D175, were identified as the residues closest to the scissile bond. The two carboxyl/carboxylate groups of these residues are within hydrogen-bonding distance of each other, and the carboxylate of D221 points to the glycosidic oxygen between sites −1 and +1. D175 also interacts with the hydroxyl group of Y169 and the guanidino group of R174. Because of these interactions, it was suggested that D175 is probably ionized, whereas D221 is protonated, and thus able to act as the proton donor. D175 was thought to ensure the correct protonation state of the catalytic acid and also, possibly, to stabilize the charged reaction transition state.[4] Mutagenesis experiments and crystallographic studies of complexes with non-hydrolyzable cello-oligosaccharides indicate that steric clashes contribute to sugar ring distortion from a chair conformation at the −1 subsite.[18,20] Structural studies of these complexes and the closely related *Humicola insolens* enzyme also indicate that one of the loops defining the tunnel is capable of conformational changes.[17,18] As a consequence of this conformational change, the interactions of D175/D221 with Y169/R174 are broken, and the side chain of S181 is pushed into the −1 site. A chain of two water molecules then links the hydroxyl of S181 to the carboxylate of D175, Figure 1. They are positioned 3.0 and 4.2 Å, respectively, from the anomeric carbon in the −1 site. Ring distortion in the −1 site is not a consequence of this conformational change.[18] In the present study, we have used a combination of site-directed mutagenesis, X-ray crystallography, molecular mechanics calculations, and enzyme mechanistic studies to elucidate the roles of the two key aspartyl residues, D221 and D175, in the active site of Cel6A.

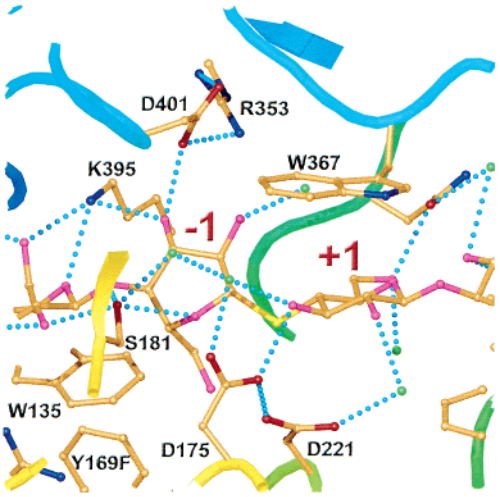

Figure 1. Binding of the substrate in the active-site tunnel of Cel6A. Some of the key residues are labeled, and hydrogen bonds are indicated by dotted lines. The figure shows the complex of the Y169F mutant with a non-hydrolyzable cellotetraose derivative (methyl 4-*S*-β-cellobiosyl-4-thio-β-cellobioside). Protein side chains are colored with carbons gold, nitrogens blue, and oxygens red. Ligand carbons are colored gold, oxygens pink, and the linking sulfur atom is yellow. Water molecules are colored green. Portions of the main chain are also shown, color-ramped from red at the N-terminus to blue at the C-terminus. The figure was created in O[59] and rendered with MOLRAY.[59]

Methods

Enzyme Kinetics. Values of k_{cat} and K_m for hydrolysis of cellotriose, cellotetraose, cellopentaose, and cellohexaose (Glc_3 to Glc_6) (Merck) in 10 mM sodium acetate buffer, pH 5.0 at 27 °C, were determined by HPLC (Waters Millipore) with RI detection as described earlier.[14,21] The substrate concentrations were 400 μM for Glc_3 and 2−250 μM for Glc_4−Glc_6 for both mutants. The kinetic constants for the wt Cel6A enzyme have been published earlier.[20,21] The pH dependence of the D175A mutant was determined at 27 °C using cellotetraose as substrate. The cellotetraose concentration in the reaction mixture was 200 μM (D175A), and the final enzyme concentration was 1.0−4.0 μM. The following buffer systems were used: glycine-HCl (pH range 1.4−3.8), sodium acetate (pH range 4.0−5.6), sodium phosphate (pH range 6.0−8.0), glycine-NaOH (pH range 9.0−10.6); the concentrations of the buffer solutions were 10 mM. In all of the measurements, samples were taken at 8−10 different time points to obtain reliable values for the initial rates. The kinetic constants were obtained from the initial velocities of the reaction curves by a nonlinear regression data analysis with the program Enzfit.[22]

Kinetics of Fluoride Ion Release. Fluoride ion liberation was followed essentially as described in ref 23. The temperature (25°C) was kept constant during measurements using a Haake temperature bath. Data were collected via a serial interface with an IBM-compatible PC using the software Hyperterminal for recording. Data were analyzed using the PC software FigP. Before initial rates of hydrolysis of α-cellobiosyl fluoride were measured, the contaminating β-anomer was

(10) Koshland, D. E. *Biol. Rev.* **1953**, *28*, 416−436.
(11) Knowles, J. K. C.; Lehtovaara, P.; Murray, M.; Sinnott, M. L. *J. Chem. Soc., Chem. Commun.* **1988**, 1401−1402.
(12) Claeyssens, M.; Tomme, P.; Brewer, C. F.; Hehre, E. J. *FEBS Lett.* **1990**, *263*, 89−92.
(13) McCarter, J. D.; Withers, S. G. *Curr. Opin. Struct. Biol.* **1994**, *4*, 885−92.
(14) Koivula, A.; Lappalainen, A.; Virtanen, S.; Mäntylä, A. L.; Suominen, P.; Teeri, T. T. *Protein Expression Purif.* **1996**, *8*, 391−400.
(15) Koivula, A.; Kinnari, T.; Harjunpaa, V.; Ruohonen, L.; Teleman, A.; Drakenberg, T.; Rouvinen, J.; Jones, T. A.; Teeri, T. T. *FEBS Lett.* **1998**, *429*, 341−6.
(16) Ståhlberg, J.; Divne, C.; Koivula, A.; Piens, K.; Claeyssens, M.; Teeri, T. T.; Jones, T. A. *J. Mol. Biol.* **1996**, *264*, 337−49.
(17) Varrot, A.; Schulein, M.; Davies, G. J. *Biochemistry* **1999**, *38*, 8884−91.
(18) Zou, J.-y.; Kleywegt, G. J.; Ståhlberg, J.; Driguez, H.; Nerinckx, W.; Claeyssens, M.; Koivula, A.; Teeri, T. T.; Jones, T. A. *Structure* **1999**, *7*, 1035−1045.
(19) Harjunpaa, V.; Teleman, A.; Koivula, A.; Ruohonen, L.; Teeri, T. T.; Teleman, O.; Drakenberg, T. *Eur. J. Biochem.* **1996**, *240*, 584−91.
(20) Koivula, A.; Reinikainen, T.; Ruohonen, L.; Valkeajarvi, A.; Claeyssens, M.; Teleman, O.; Kleywegt, G. J.; Szardenings, M.; Rouvinen, J.; Jones, T. A.; Teeri, T. T. *Protein Eng.* **1996**, *9*, 691−9.
(21) Teleman, A.; Koivula, A.; Reinikainen, T.; Valkeajarvi, A.; Teeri, T. T.; Drakenberg, T.; Teleman, O. *Eur. J. Biochem.* **1995**, *231*, 250−8.
(22) Marquart, D. W. *J. Soc. Ind. Appl. Math.* **1963**, *11*, 431−441.
(23) Konstantinidis, A.; Sinnott, M. L. *Biochem. J.* **1991**, *279*, 587−93.

Table 1. Kinetic Parameters for the wt Cel6A and Mutant Enzymes D221A and D175A on Cello-oligosaccharides (Glc_n, $n = 4-6$) Measured in 10 mM Sodium Acetate Buffer, pH 5.0 at 27 °C[a]

	wt Cel6A			D221A	D175A		
substrate	k_{cat} (s^{-1})	K_m (μM)	k_{cat}/K_m ($s^{-1}\,\mu M^{-1}$)	k_{cat} (s^{-1})	k_{cat} (s^{-1})	K_m (μM)	k_{cat}/K_m ($s^{-1}\,\mu M^{-1}$)
Glc_3	0.06 ± 0.01	17 ± 5	0.004 ± 0.002	≤ 0.0001	≤ 0.0003	nd	
Glc_4	4.1 ± 0.5	2.6 ± 0.5	2.0 ± 0.5	≤ 0.0012	0.0013 ± 0.0010	4 ± 1	0.0003 ± 0.0004
Glc_5	1.1 ± 0.2	1.3 ± 0.4	0.8 ± 0.5	≤ 0.0010	0.025 ± 0.001	1.4 ± 0.7	0.02 ± 0.01
Glc_6	14 ± 2	14 ± 6	1.0 ± 0.7	≤ 0.0007	0.020 ± 0.001	nd	

[a]Owing to low activity, K_m values could not be measured for the D221A mutant. Kinetic constants were calculated by a nonlinear regression data analysis program (Enzfit), which also gives the standard deviation. nd = not determined.

completely hydrolyzed using Cel7A.[24] In the case of β-cellobiosyl fluoride, the level of substrate degradation after deacetylation was tested with the fluoride ion probe by comparing fully hydrolyzed substrate (using *T. reesei* Cel6A for degradation) with the starting material. Batches with more than 6% degradation were not used for kinetic experiments. Enzyme concentrations for α-cellobiosyl fluoride measurements were 3.85 (D175A) and 7.4 μM (D221A), and for β-cellobiosyl fluoride measurements they were 3.85 and 0.96 μM. Hydrolysis of 1-fluorocellobiosyl fluoride (1 mM) by wt Cel6A (8 μM) was monitored for 5 days, with the electrode being recalibrated for each reading.

Solvent Isotope Effect on the Hydrolysis of Cellotriose by Wild-type Cel6A. The solvent isotope effect on k_{cat} was measured with 0.300 mM substrate ($20 \times K_m$) at 37.0 °C. Initial rates of three separate reactions in H_2O and D_2O were obtained by analysis of liberated glucose with high-performance anion exchange chromatography, using pulsed amperometric detection, under the conditions specified by the manufacturer of the equipment (Dionex, Sunnyvale, CA). To eliminate complexities of interpretation arising from solvent isotope effects on essential ionizations, the rate in H_2O was measured at the pH optimum of the enzyme (4.5) in 10 mM sodium acetate buffer. The rate in D_2O was measured at the same buffer ratio as in H_2O, where it gave a pH of 4.50. Because the likely critical ionizations arise from carboxylic acid residues, we make the usual assumption that the solvent isotope effect on ionizations of the same chemical type is constant.

Ligand-Binding Studies. Binding of 4-methylumbelliferyl-β-glucoside, -cellobioside, and -cellotrioside [MeUmb(Glc), MeUmb$(Glc)_2$, and MeUmb$(Glc)_3$] in 50 mM sodium acetate buffer, pH 5.0 at 16 °C, was studied by direct fluorescence quenching titrations as described before.[25] Fluorescence was measured with an Aminco SPF-500 spectrofluorometer equipped with a thermostated cuvette holder. Excitation was at 318 nm (spectral bandwith 2 nm), and the emission was measured at 360 nm with a bandwidth of 15, 20, or 40 nm. Cellobiose and cellotriose (Merck) were used as competitive ligands for MeUmb$(Glc)_2$ (indicator) in the displacement titrations. The dissociation constants for different oligosaccharides were obtained by nonlinear least-squares fitting to the fluorescence data as described in ref 20.

Crystallographic Analysis. Data collection and refinement statistics are listed in Tables S1 and S2 in the Supporting Information. Coordinates and structure factors have been deposited at the PDB with codes 1HGY and 1HGW.

Modeling of Enzyme-Ligand Complexes. The protein-modeling package BRAGI[26] and the molecular-mechanics program AMBER 4.0[27] were used for simulations of the enzyme-ligand complexes. The AMBER all-atom force field[28] together with the GLYCAM force field for saccharides [29] and additional parameters for the reaction intermediates were used in these calculations. These additional parameters were fitted to reproduce data from ab initio calculations with Gaussian 94[30] at the B3LYP/6-31G* level. A two-stage restrained electrostatic potential fit method was used to obtain atomic point charges.[31] All simulations were based on a number of experimental structures determined by X-ray crystallography for the wild-type Cel6A and two mutants.[4,18] All histidines, except H266, were assumed to be protonated at both nitrogens in accordance with the pH value of 5.0 used in most experiments. H266 was deemed to be protonated only at Nϵ, after taking into account its structural environment. All carboxylic acid side chains were negatively charged in the enzyme-ligand complex simulations, except E107, D170, D419, and D221, which were kept protonated. Initial ligand position and chain directionality for the force field calculations were derived from the X-ray structure of the Y169F/$(Glc)_2$-*S*-$(Glc)_2$ complex.[18] The force field calculations were carried out with explicit TIP3P water molecules[32] at a dielectric constant $\epsilon = 1$ and a cutoff distance of 9 Å for the nonbonded interactions. During the molecular dynamics simulations, the SHAKE algorithm[33] was used to constrain the covalent bonds to their equilibrium bond length. Only the atoms within a 16 Å radius around the glycosidic oxygen between -1 and $+1$ site were allowed to move during these simulations. The structures were energy-minimized and then equilibrated by molecular dynamics for 50 ps at 298 K with an integration interval of 1 fs. After equilibration, a trajectory over 500 ps was saved every 1 ps. The resulting structural ensembles were compared to X-ray structures, and trajectories were analyzed for interactions of mechanistic importance using the CARNAL module of the AMBER package.[27]

Results

Production and Purification of the Mutant Proteins. The mutant proteins were produced in *T. reesei* strains devoid of the wt Cel6A gene for the D221A mutant and both the Cel6A and the Cel5A genes for the D175A mutant. Analysis of their enzymatic properties was carried out using protein preparations with no or minute activity on substrates diagnostic for the endoglucanases.[14]

Catalytic Effects of the Mutations. The catalytic constants for the action of wt Cel6A and the two mutants on soluble cello-oligosaccharides are presented in Table 1. The values of k_{cat} of

(24) Becker, D.; Johnson, K. S.; Koivula, A.; Schulein, M.; Sinnott, M. L. *Biochem. J.* **2000**, *345 Pt 2*, 315−9.
(25) van Tilbeurgh, H.; Pettersson, G.; Bhikabhai, R.; De Boeck, H.; Claeyssens, M. *Eur. J. Biochem.* **1985**, *148*, 329−34.
(26) Schomburg, D.; Reichelt, J. *J. Mol. Graphics* **1988**, *6*, 161−165.
(27) Pearlman, D. A.; Case, D. A.; Caldwell, J. C.; Seibel, G. L.; Singh, U. C.; Weiner, P.; K.P.A. *AMBER*, 4.0 ed.; University of California: San Francisco, 1991.
(28) Cornell, W. D.; Cieplak, P.; Bayly, C. I.; Gould, I. R.; Merz, K. M.; Ferguson, D. M. S.; D.C.F., T.; Caldwell, J. W.; Kollman, P. A. *J. Am. Chem. Soc.* **1995**, *117*, 5179−5197.
(29) Woods, R. J.; Dwek, R. A.; Fraser-Reid, B. *J. Phys. Chem.* **1995**, *99*, 3832−3840.
(30) Frisch, M. J.; Trucks, G. W.; Schlegel, H. B.; Gill, P. M. W.; Johnson, B. G.; Robb, M. A.; Cheeseman, J. R.; Keith, T.; Petersson, G. A.; Montgomery, J. A.; Raghavachari, K.; Al-Laham, M. A.; Zakrzewski, V. G.; Ortiz, J. V.; Foresman, J. B.; Cioslowski, J.; Stefanov, B. B.; Nanayakkara, A.; Challacombe, M.; Peng, C. Y.; Ayala, P. Y.; Chen, W.; Wong, M. W.; Andres, J. L.; Replogle, E. S.; Gomperts, R.; Martin, R. L.; Fox, D. J.; Binkley, J. S.; Defrees, D. J.; Baker, J.; Stewart, J. P.; Head-Gordon, M.; Gonzalez, C.; A., P. J. *Gaussian 94*, revision B.3; Gaussian, Inc: Pittsburgh, PA, 1995.
(31) Bayly, C. I.; Cieplak, P.; Cornell, W. D.; Kollman, P. A. *J. Phys. Chem.* **1993**, *97*, 10296−10280.
(32) Jorgensen, W. L.; Chandrasekhar, J.; Madura, J. D.; Imey, R.; Klein, M. *J. Chem. Phys.* **1983**, *79*, 926−935.
(33) Ryckaert, J. P.; Cicotti, G.; Berendsen, H. J. C. *J. Comput. Phys.* **1977**, *23*, 327−341.

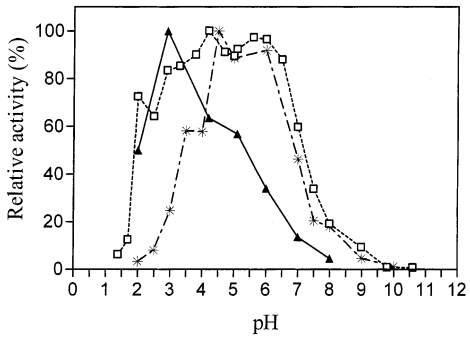

Figure 2. pH-activity profiles of wt Cel6A (- - □ - -), Y169F (- - ∗ - -) (data from ref 20), and D175A (- - ▲ - -) mutant enzymes represented as relative activities. The activities were measured at 27 °C at constant cellotetraose concentration, which was approximated as saturating concentration. The absolute activity value of the D175 mutant at pH 5.0 corresponds to about 0.03% of the Cel6A wild-type activity.

Table 2. Kinetic Parameters for the Hydrolysis of Cellobiosyl Fluorides, in 0.100 M Sodium Acetate Buffer, pH 5.0 at 25 °C

enzyme	α-cellobiosyl fluoride[a]	β-cellobiosyl fluoride
wild-type	$k_{cat} = 0.54\ s^{-1}$	$k_{cat} = 4.0\ s^{-1}$
	$K_m = 2.35$ (mM)[2]	$K_m = 0.15$ mM
D221A	$k_{cat} < 1.3 \times 10^{-5}\ s^{-1}$	$k_{cat} = 0.103\ s^{-1}$
	K_m: not determined	$K_m = 1.3$ mM
D175A	$k_{cat} = \sim 3 \times 10^{-4}\ s^{-1}$	$k_{cat} = 0.013\ s^{-1}$
	K_m: not determined	$K_m = 0.18$ mM

[a] Kinetic parameters calculated for a bimolecular reaction.[24]

the D221A mutant indicate almost complete loss of activity, whereas the D175A mutant retains some activity on longer oligosaccharides. Owing to its low activity, the K_m values could not be accurately calculated for the D221A mutant. Essentially no changes were observed in the K_m values for the D175 mutant on cellotetraose or cellopentaose (Table 1). The specificity constant (k_{cat}/K_m) of D175A is over 6000-fold lower than that of wt Cel6A on cellotetraose, whereas only a 40-fold reduction is observed on a longer substrate, Table 1.

Figure 2 shows the pH dependence of the reaction rate for cellotetraose degradation for wt Cel6A, the D175A mutant, and the Y169F mutant that was earlier shown to influence the pH behavior of Cel6A.[20] The data were measured at saturating substrate concentrations based on our earlier kinetic data on wt Cel6A.[20] The activity of the D175A mutant was found to be lower than the activity of wt Cel6A over the whole pH range studied, but the effect is more pronounced for the basic limb.

Determination of the activities of the mutant enzymes on the α- and β-cellobiosyl fluorides revealed a 40-fold reduction in k_{cat} for the hydrolysis of the β-anomer by the D221A mutant, but a >40 000-fold reduction in k_{cat} for the hydrolysis of the α-anomer (Table 2). In contrast, the D175A mutant shows a large, similar reduction in k_{cat} for hydrolysis of both anomers (1800-fold α, 300-fold β).

Even with 8 μM wt enzyme, fluoride ion liberation from 1-fluorocellobiosyl fluoride was only ~6 times faster than the blank rate; this corresponds to a k_{cat} of $\sim 2 \times 10^{-6}\ s^{-1}$, if the enzyme is saturated .

The solvent kinetic isotope effect for the hydrolysis of cellotriose by wt Cel6A was only slightly above 1 [$^{D2O}(V) = 1.16 \pm 0.14$].

Binding Properties of the Mutant Proteins. The binding constants for a number of different ligands to wt Cel6A and the two mutants are given in Table 3. Neither of the mutations introduced to the active site of Cel6A led to any major changes in its binding behavior.

Table 3. Dissociation Constants for the Binding of Carbohydrates to Wild-type Cel6A, D221A, and D175A Mutants, in 50 mM Sodium Acetate Buffer, pH 5.0 at 16 °C[a]

	K_d (μM)		
ligand	wt Cel6A	D221A	D175A
$MeUmb(Glc)_1$	18[b]	100	nd
$MeUmb(Glc)_2$	2.6	5	0.8
$MeUmb(Glc)_3$	0.1[c]	0.1	0.2
Glc_2	1400	330	1100
Glc_3	15	2.9	4.5

[a] nd = not determined. [b] The uncertainty in all measured K_d values is estimated to be 15% on the basis of four repeated experiments. [c] The measurement with wt Cel6A on $MeUmb(Glc)_3$ was performed at 8 °C.

Structures of the D221A and D175A Mutants. The two Cel6A mutants crystallize in different space groups, but both contain two molecules per asymmetric unit. The structures that we report, therefore, provide four views of the protein. The overall structures of the mutants are very similar, except for one of the tunnel-defining loops, corresponding to residues 172−182. The mutants have four different conformations that affect the active site and the −1 binding site, in particular (Figures 3 and 4). They range from molecule A of D221A, where the tunnel is squeezed at the −1 site and is essentially identical to the Y169F/$(Glc)_2$-*S*-$(Glc)_2$ complex structure described in ref 18, Figures 1 and 3b, to an almost open active site in molecule A of D175A, Figure 3c. Molecule B of D175A has the conformation first seen in the wt apo-enzyme, Figure 3b, whereas D221A molecule B is somewhat more open as previously observed in the wild-type/*m*-iodobenzyl β-D-glucopyranosyl-β(1,4)-D-xylopyranoside complex structure.[18] In the squeezed tunnel of D221A molecule A, the conformational change breaks the interaction of D175 with R174, as previously observed in the Y169F/$(Glc)_2$-*S*-$(Glc)_2$ structure.[18] However, the side chain of D175 has a different conformation, probably as a result of the D221A mutation. The remaining residues in the 172−182 loop adopt a conformation very similar to the one observed in the Y169F/$(Glc)_2$-*S*-$(Glc)_2$ structure. In the B molecule, the D175/R174 interaction is also broken, but the loop is more open, and its density is less clearly defined. This, in turn, results in higher average temperature factors (see Table S2 in the Supporting Information).

In the D175A crystal structure, one of the molecules has a much more open active site as a result of the largest conformational change in the 172−182 loop that we have so far observed in any Cel6A structure. In particular, the −1, +1, and +2 sites are more exposed to the solvent, whereas the side chains forming the −2 site remain essentially unchanged, Figures 3c and 4.

Molecular Modeling Based on the Experimental 3-D Structures of Cel6A. To obtain a more detailed picture of the reaction pathway of Cel6A, a series of possible reaction intermediates was modeled starting with different experimental structures of the wild-type Cel6A or its mutants.

A model for the ground-state binding situation with cellotetraose was derived, starting from the Y169F/$(Glc)_2$-*S*-$(Glc)_2$ complex structure,[18] that is, the most closed loop structure, with the −1 site sugar modeled in different skew-boat and chair

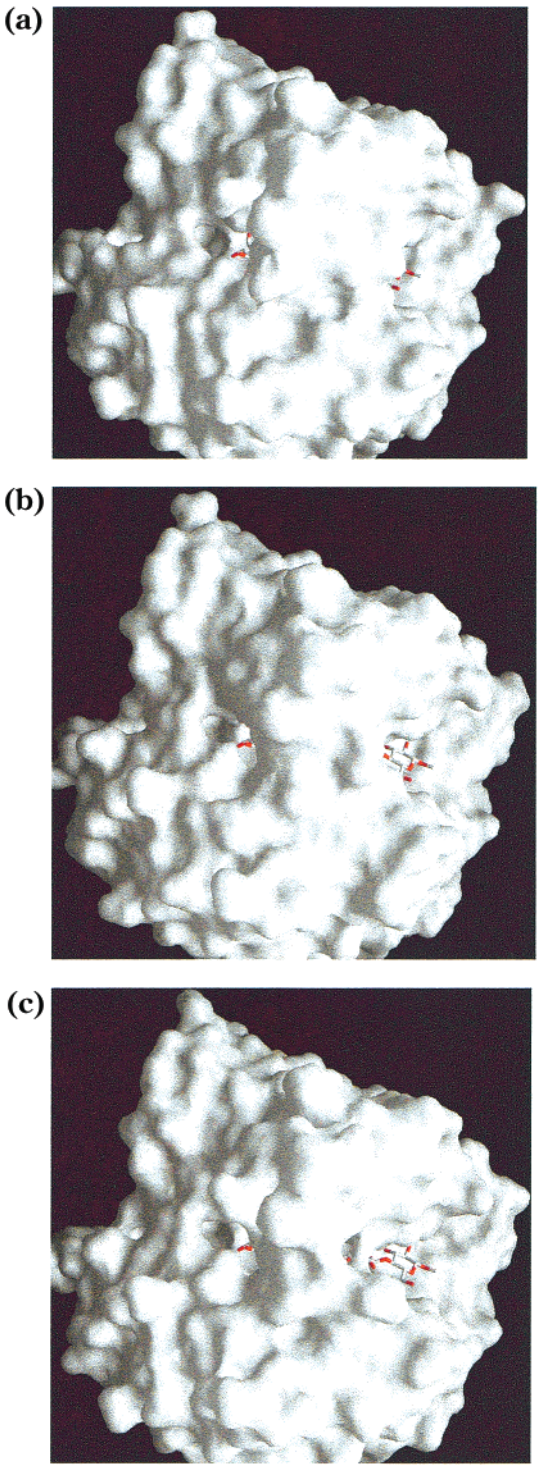

Figure 3. Molecular surfaces of the Cel6A tunnel region: (a) wt Apo. (b) Y169F in complex with $(Glc)_2$-*S*-$(Glc)_2$. (c) D175A molecule A. The $(Glc)_2$-*S*-$(Glc)_2$ molecule has been modeled on the basis of the Y169F mutant complex structure. The figures were made with GRASP.[60]

conformations. Here, the sulfur linkage of the ligand in the experimentally determined structure was changed to an oxygen linkage, and the mutation Y169F was reverted to the wt tyrosyl-residue prior to the simulation. During the course of the 500 ps MD simulation, the movable atoms showed an rmsd of 1.09 ± 0.04 Å to the X-ray structure with a maximal deviation of 1.19 Å. The sugar in the −1 site remained in the skew-boat conformation ($^2S_0$). MD simulations carried out with different initial conformations of the −1 sugar all converged to the

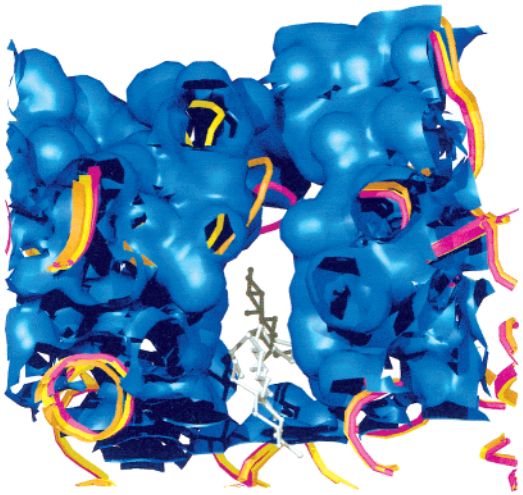

Figure 4. Conformational changes that occur in one of the tunnel-defining loops in Cel6A. D175A molecule A is colored yellow, the apo wild-type molecule is gold, and the Y169F in complex with $(Glc)_2$-*S*-$(Glc)_2$ is magenta. The $(Glc)_2$-*S*-$(Glc)_2$ molecule from the Y169F mutant complex is also included. The surface is derived from the most open active site structure D175A molecule A.

experimentally observed $^2S_0$ conformation, which indicates that it is strongly stabilized by the environment. In the starting structure, D175 was defined as charged, and the proposed catalytic acid D221 was protonated, acting as a hydrogen bond donor to D175. During the simulation, the side chain of D221 remained hydrogen bonded to the side chain of D175, and its closest oxygen had a distance of 4.0 ± 0.3 Å to the glycosidic oxygen to be protonated during the reaction. The closest approach of the carboxyl proton to the glycosidic oxygen was 3.07 Å (Figure 5a).

In the next MD simulation, the bridging proton between D175 and D221 was shifted to the other oxygen of D221. Upon giving up its hydrogen bond to D175, the side chain of D221 rotated through its χ_1 angle, thus breaking the contact with D175. This brought the protonated oxygen of D221 closer to the glycosidic oxygen, 3.3 ± 0.3 Å, over the first 300 ps, after which the hydrogen bond between D175 and D221 was formed again. The approach of the carboxyl hydrogen of D221 to the glycosidic oxygen was much closer than 2.0 Å. This close approach, and a good positioning of the carboxyl group with the nonbonding, doubly occupied orbital of the glycosidic atom of the −1 site, is consistent with a facile proton transfer, Figure 5b. The side-chain conformation of D221 observed in this simulation is practically identical to that observed for the corresponding residue in the structure of the family 6 endoglucanase, E2 from *Thermomonospora fusca*.[34] In the E2 structure, however, the loop carrying the residue corresponding to our D175 is turned away from the active site, and no contact is formed between the two aspartyl residues.

Independently of whether the reaction passes through an oxycarbenium cation as the reactive intermediate, or via an S_N2-type transition state, the C1 atom will become trigonal. The main difference between an S_N1 reactive intermediate and an S_N2 transition state is reflected in the distance of the two ligands to the C1 atom. We have chosen to model the transition state using an oxycarbenium cation. A model of this intermediate

(34) Spezio, M.; Wilson, D. B.; Karplus, P. A. *Biochemistry* **1993**, *32*, 9906−16.

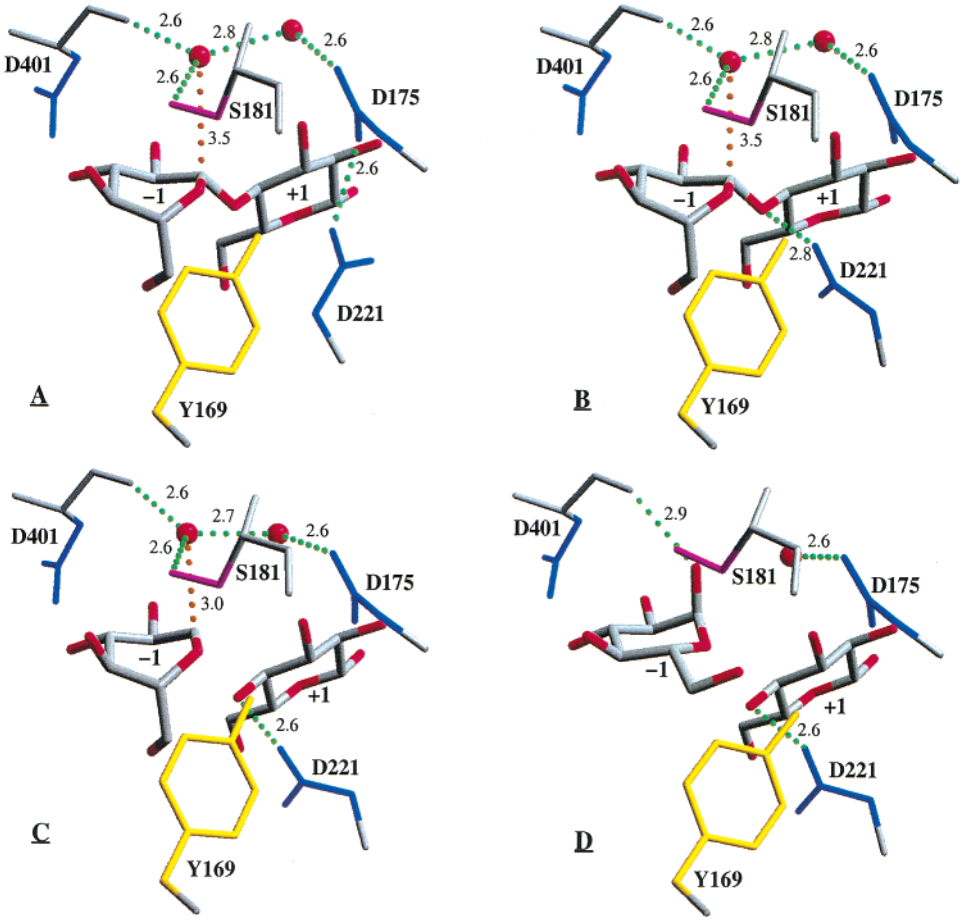

Figure 5. Snapshots of the molecular dynamics simulations of the proposed catalytic states. Only the residues in the −1 and +1 sites are shown. All hydrogens and the backbone atoms of Y169, D175, and D221 are omitted for clarity. Important hydrogen bonds are shown as green dots, and the interaction between water and C1, important for the nucleophilic attack, is shown in orange. The models of different reaction states show (a) the ground state with the −1 site sugar in a skew-boat conformation ($^2S_0$), (b) the ground state with the D221 side chain rotated toward the glycosidic oxygen, (c) an oxycarbenium ion intermediate modeled in a boat conformation (^{2,5}B) as an analogue to the transition state, and (d) two sugars of the reaction products (α-cellobiose in the −1 and −2 sites and β-cellobiose in the +1 and +2 sites).

was built starting from the ground-state structure, and the geometry of the oxycarbenium cation was derived by ab initio calculations with Gaussian 94.[30] To "scan" the active site for a basic residue, which could activate a water molecule for the nucleophilic attack at the C1 carbon, different initial conformations of the glycosidic bond between the −2 and −1 sites and of the ring in the −1 site were used for MD simulations. Most of these simulations converged to structures very similar to the ground-state model described above and the X-ray structure of the Y169F/$(Glc)_2$-*S*-$(Glc)_2$ complex (rmsd < 0.5 Å). None of the simulations suggested an amino acid residue positioned to act as the catalytic base. However, some of the models revealed water molecules that could attack the C1 of the oxycarbenium cation. Although in some of these models the water is positioned on the side that would lead to a β-product, the energetically most favorable model establishes geometry suitable to form the expected α-product. This model shows the cation in a ^{2,5}B conformation. The distance from C1 to the water atom during the 500 ps MD is 3.1 ± 0.2 Å as compared to 3.6 ± 0.2 Å in the ground-state simulation. This water is fixed by the S181 side chain and the D401 backbone carbonyl and is connected to the D175 side chain via a second water molecule (Figure 5c). The modeling experiment is, therefore, in good agreement with the local water structure observed in the Y169/$(Glc)_2$-*S*-$(Glc)_2$ complex structure of ref 18, Figure 1. After the bond cleavage in the simulation, the sugar ring relaxed back to the chair conformation, and the product was pushed slightly out of the active site (Figure 5d).

Discussion

Active Site Conformational Changes. The key catalytic residues in all inverting and most retaining glycoside hydrolases are a pair of acidic residues from the protein.[35] In inverting enzymes, the carboxylate group of one residue acts as a base, the carboxyl group of the other as an acid, to promote direct displacement of the leaving aglycone by water.[13] Recently, it has become increasingly clear that another crucial element in the catalytic mechanism of cellulases is the ring distortion at the −1 site.[8,9,18,20,36] The crystal structure of *T. reesei* Cel6A revealed a pair of aspartyl side chains in its active site, D175 and D221, that were at hydrogen-bonding distance from each other and on the same side of the scissile bond.[4] The environment suggested that D221 is protonated, and it was proposed to act as the acid catalyst. Subsequent crystallographic and mutagenesis studies of wt and Y169F enzyme revealed a more

(35) Davies, G.; Sinnott, M. L.; Withers, S. G. In *Comprehensive biological catalysis*; Sinnott, M. L., Ed.; Academic Press: London, 1998; Vol. I, pp 119−208.
(36) Sulzenbacher, G.; Driguez, H.; Henrissat, B.; Schulein, M.; Davies, G. J. *Biochemistry* **1996**, *35*, 15280−7.

complex active site. The complementary structural, mutagenesis, and substrate binding studies were interpreted to suggest that Y169 helps to distort the glucose ring into a more reactive conformation.[20] Further wt and Y169F structures in complex with a non-hydrolyzable cellotetraose-like ligand, methyl 4-*S*-*β*-cellobiosyl-4-thio-*β*-cellobioside, showed that the glucosyl unit in the −1 site is indeed distorted into a ^2S_O conformation.[18] The ligand conformations, however, are identical in both enzymes and, hence, not a result of the tyrosyl-residue acting alone. The mutant structure, though, undergoes a conformational change in one of the principal tunnel-forming loops. As a result, the interaction of D175 with R174 is broken, whereas the D175/D221 interaction is maintained. Also, a string of water molecules becomes visible, linking the carboxylate of D175 to the anomeric carbon C1 at the −1 site, Figure 1. One water molecule, forming a hydrogen bond with D175, is positioned 4.2 Å from C1. The other is at a distance of 3.0 Å and correctly positioned to produce the α-glucosyl residue upon catalysis. The latter water molecule also interacts with the hydroxyl group of S181 (a residue that moves ∼6 Å as a result of the conformational change) and the main-chain carbonyl of residue 401. However, there is no interaction of this potentially catalytic water with an enzyme residue, which serves as a base. The proposed acid-catalyst D221, on the other hand, is closely positioned to the sulfur in the glycosidic linkage between the −1 and +1 sites. However, the interaction geometry suggests that a hydrogen bond is maintained between the carboxylate groups of D175 and D221 in the Y169F/$(Glc)_2$-*S*-$(Glc)_2$ complex (Figure 1). This may be a consequence of the increased van der Waals radius of the sulfur in the glycosidic linkage. The distortion of the glucosyl unit in the −1 site is not a result of the conformational change, because essentially the same ligand structure was present in the complex with the wt enzyme, which did not show the loop adjustment.[18]

The *T. reesei* cellobiohydrolases Cel6A and Cel7A are known to act on crystalline cellulose. To do this, they must first remove a cellulose chain from the crystal, which requires energy. Some time ago, Sinnott and co-workers[37] proposed that the cellobiohydrolases are molecular machines that coupled the energy required for crystallite disruption to the energy released on glycoside hydrolysis. In support of this idea, it was later shown that the energetic coupling of crystallite disruption to glucan hydrolysis was reversible; radiolabeled cellobiose was incorporated into *Acetobacter xylinum* cellulose by Cel6A under conditions where the hydrolysis in free solution was essentially irreversible.[38] A key feature of known molecular machines[39] is that the respective molecules exist in two (or more) significantly different conformational states. The different conformations observed around the active site of Cel6A are directly coupled to the catalytic events and may contribute to the movement of the glucan chains in the active site tunnel of the enzyme. Even these observations are in agreement with the molecular machine hypothesis.

D221 Is the Catalytic Acid. Hitherto, all of the data obtained on *T. reesei* Cel6A and the other enzymes in this family support the role of D221 as the catalytic acid. The D221A mutant was catalytically inactive on oligosaccharides of different length, although its binding properties are identical to those of the wt enzyme (Tables 1, 3). Data supporting the role of D221 as the proton donor were also obtained by using α- and *β*-cellobiosyl fluorides (Table 2). The fluoride ion does not require complete protonation for a C−F bond to be cleaved in water, because the pK_a of H−F is 3.2 and F^- is unprotonated in aqueous solution, even though it is strongly hydrogen bonded (vide infra). Consequently, mutation of the proton donor should have a modest effect on the hydrolysis of *β*-cellobiosyl fluoride. In the case of the D221A mutation, a 40-fold effect was nevertheless observed. It is possible that this is a consequence of interactions between the catalytic residues. For example, because of their proximity, the D221A mutation may have a major effect on the properties of D175, which in turn may modify the activity.

There is a requirement for the departing fluoride ion to be solvated by hydrogen bonding, even though it does not require full protonation. In the case of oligosaccharides and polysaccharides, however, the leaving group absolutely requires protonation during departure, because its pK_a is in the region of 13−14. Therefore, the much greater effect of the D221A mutation on the hydrolysis of these substrates confirms the assignment of D221 as the acid catalyst. Furthermore, the D221A mutant was completely inactive toward α-cellobiosyl fluoride. In general, inverting glycosidases hydrolyze glycosyl fluorides of the "wrong" anomeric configuration by a resynthesis−hydrolysis mechanism[40] illustrated in Figure 6. In the first step, two molecules of the fluoride are condensed by the enzyme in a reversed-protonated state (acid catalyst deprotonated and base catalyst protonated) to yield a new glycosidic link, which is then hydrolyzed by the normal pathway. After a recent reevaluation of earlier data, *T. reesei* Cel6A seems to hydrolyze α-cellobiosyl fluoride by the Hehre mechanism.[24,37,41] A key feature of the first, transglycosylation, step of this mechanism is that the acid-catalytic group, as its conjugate base, deprotonates the hydroxyl group of the second saccharide molecule. If this catalytic group is removed, as in the mutant D221A, the transglycosylation should cease, and this is indeed observed.

The experimental structures and the simulations presented here, as well as data obtained with other family 6 cellulases from *Cellulomonas fimi*,[41,42] *Thermomonospora fusca*,[43] and *Humicola insolens*,[17,44,45] are also consistent with the role of D221 as the catalytic acid. The molecular dynamics simulations suggest that breaking the hydrogen bond contact between D175 and D221 may induce a new, catalytically relevant side-chain conformation of D221. This conformation, experimentally observed in both the *T. fusca* E2[34] and the *H. insolens* Cel6A structures,[17,44] brings the protonated carboxyl-oxygen of D221 closer to the glycosidic oxygen.

The Role(s) of D175. Some residual activity (2−3%) on barley *β*-glucan was measured for the D175A mutant enzyme produced in *Saccharomyces cerevisiae*, while the D221A mutant

(37) Konstantinidis, A. K.; Marsden, I.; Sinnott, M. L. *Biochem. J.* **1993**, *291*, 883−8.
(38) Sweilem, N. S.; Sinnott, M. L. In *Carbohydrases from Trichoderma and other microorganisms*; Claeyssens, M., Nierinckx, W., Piens, K., Eds.; Royal Society of Chemistry: London, 1998; pp 13−20.
(39) Banting, G.; Higgins, S. J. *Tetrahedron Lett.* **2000**, *28*, 35.
(40) Hehre, E. J. In *Enzymatic degradation of insoluble carbohydrates*; Saddler, J. N., Penner, M. H., Eds.; ACS Symposium Series 618; American Chemical Society: Washington, DC, 1995; pp 68−78.
(41) Damude, H. G.; Ferro, V.; Withers, S. G.; Warren, R. A. *Biochem. J.* **1996**, *315*, 467−72.
(42) Damude, H. G.; Withers, S. G.; Kilburn, D. G.; Miller, R. C., Jr.; Warren, R. A. *Biochemistry* **1995**, *34*, 2220−4.
(43) Wolfgang, D. E.; Wilson, D. B. *Biochemistry* **1999**, *38*, 9746−9751.
(44) Varrot, A.; Hastrup, S.; Schulein, M.; Davies, G. J. *Biochem. J.* **1999**, *337*, 297−304.
(45) Davies, G. J.; Brzozowski, A. M.; Dauter, M.; Varrot, A.; Schulein, M. *Biochem. J.* **2000**, *348 Pt 1*, 201−7.

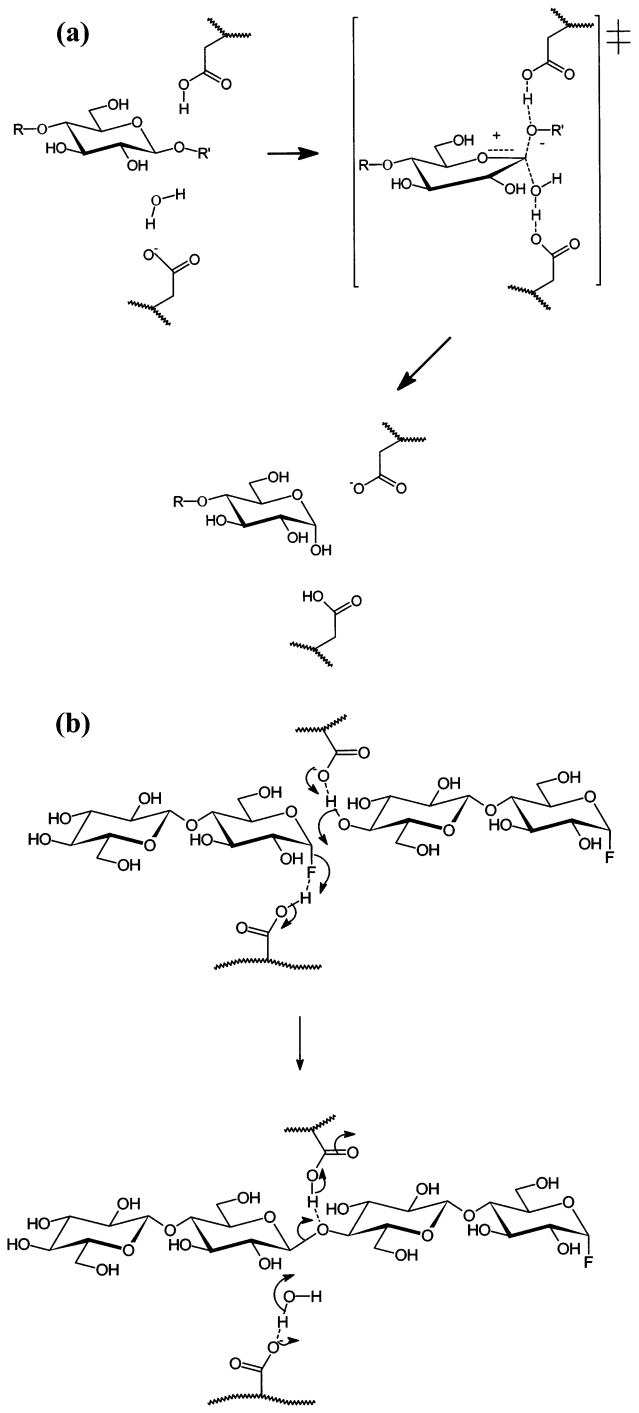

Figure 6. (a) General mechanism for an inverting β-glucanase. (b) Hehre mechanism for hydrolysis of the "wrong" glycosyl fluoride applied to the reaction with α-cellobiosyl fluoride. "Exploded" transition states will be involved in both cases, but the degree of bonding to leaving group and nucleophile will not necessarily be the same, nor need the leaving group, nucleophilic, and anomeric carbon to be strictly collinear. Additionally, the development of partial double bond character in O5−C1 may not be synchronous with the development of partial positive charge on C1. In this particular case, the reactive conformation of the pyranose ring in the subsite −1 is $^2S_0$, not the $^4C_1$ conformation shown here.

was totally inactive on this substrate (our unpublished data). When produced in *T. reesei*, the D175A mutant showed very little activity on oligosaccharides, particularly on cellotetraose, without major changes in its substrate binding properties (Tables 1 and 3). These data indicate that D175 is catalytically significant. However, the residual activities observed would seem to argue against a role as the catalytic base. The activity of the mutant on the cellobiosyl fluorides is also informative. If D175 were a simple catalytic base, the mutation should have a large effect on the hydrolysis of the β-fluoride. In the case of the α-fluoride, the first step of its hydrolysis is a transglycosylation, which involves the active site residues in their reverse-protonated state. Here, the departure of the fluoride ion does not require a relatively strong acid; water as a H-bond donor ought to suffice to allow for solvolysis. Therefore, eliminating the group, now acting as the catalytic acid, should have only a modest effect. The D175A mutation, however, had similar, large, effects on the hydrolysis of both fluorides (Table 2), and, therefore, D175 cannot be the catalytic base in the normal sense. Its removal clearly decreases the pK_a of the catalytic acid, as shown in Figure 2 by the shift in the pH-rate profile.

The effect of substitution of the anomeric hydrogen of β-cellobiosyl fluoride substrate with a second fluorine suggests that the transition state is exceptionally electron-deficient, so that D175 may stabilize electrostatically. Fluoroglycosyl fluorides, in general, are comparatively efficiently hydrolyzed by many glycosidases.[46] They are slower substrates than glycosyl fluorides, but by factors rarely approaching the 1000 (α) or 30 000 (β) seen in spontaneous hydrolysis. We have suggested that the (V/K) ratio, converted to a free energy ($\Delta\Delta G^{\ddagger} = -RT \ln\{(k_{cat}/K_m)_F/-(k_{cat}/K_m)_{F2}\}$), can be used as a measure of charge development at the first transition state.[23,37,47] The 1-fluorocellobiosyl fluoride was synthesized via the action of xenon difluoride on the glycosyl diazirine (see Supporting Information) but proved to be only a barely detectable substrate. The K_m values observed with other inverting glycosidases acting on glycosyl fluoride and 1-fluorosyl fluoride are very similar to each other. Assuming that this is also the case with Cel6A permits us to extract a k_{cat} value from the hydrolysis experiment (conducted at [S] ≈ $7K_m$), and then to calculate a $\Delta\Delta G^{\ddagger}$ from the k_{cat} values alone. The $\Delta\Delta G^{\ddagger}$ value obtained in this way was ∼36 kJ mol^{-1}, which is higher than the equivalent value ($-RT \ln 3000 = 25$ kJ mol^{-1}) for spontaneous hydrolysis. This indicates a higher degree of charge buildup in the transition state for Cel6A catalysis than that for spontaneous hydrolysis.

Provided $\Delta\Delta G^{\ddagger}$ values are based on k_{cat}/K_m, this conclusion is independent of the assumption made in our early work that the effect of the second fluorine is to destabilize the oxocarbenium ion. AM1 calculations (Bernet, B.; Vasella, A., unpublished) now indicate that α-fluorine substitution, in fact, stabilizes oxocarbenium ions. Thermochemical measurements of Rüchardt's group[48,49] suggest rather that ground-state stabilization is the source of the inertness of the fluoroglycosyl fluorides. Additional F−F and O−F anomeric interactions could account for ∼65 kJ mol^{-1} stabilization in the difluorides. Nonetheless, because in comparisons between different enzyme systems based on k_{cat}/K_m the ground state is the same, we can still take $\Delta\Delta G^{\ddagger}$ as a measure of progress toward the oxocarbenium ion, whether the effect used to measure such progress

(46) Sinnott, M. L. In *Recent advances in carbohydrate bioengineering*; Gilbert, H. J., Davies, G. J., Henrissat, B., Svensson, B., Eds.; Royal Society of Chemistry: London, 1999; pp 45−61.
(47) Konstantinidis, A. K.; Sinnott, M. L.; Hall, B. G. *Biochem. J.* **1993**, *291*, 15−17.
(48) Rakus, K.; Verevkin, S. P.; Peng, W. H.; Beckhaus, H.-D.; Ruchardt, C. *Liebings Ann.* **1995**, 2059−2067.
(49) Schaffer, F.; Verevkin, S. P.; Rieger, H. J.; Beckhaus, H. D.; Ruchardt, C. *Liebigs Ann.* **1997**, 1333−1334.

arises from loss of stabilizing ground-state geminal interactions or oxocarbenium ion destabilizing interactions.

The exceptionally highly charged transition state of this enzyme may require additional electrostatic stabilization. The electrostatic interaction of D175 with the ring oxygen in the −1 site at the transition state could provide such stabilization. The distance between the −1 sugar ring oxygen and the closest carboxylate oxygen of D175 in the structure of the Y169F/$(Glc)_2$-*S*-$(Glc)_2$ complex is only 4.5 Å, and there are no shielding atoms in between. Residue D175 is, therefore, suitably positioned to provide such electrostatic stabilization. The large effect of the D175A mutation on the hydrolysis of both fluorides then becomes easier to understand. Similar interactions have been proposed on theoretical grounds,[50] and some experimental support for them has been found in model systems.[51]

Role of D401? On the basis of its strict conservation and its position relative to the catalytic acid, it has been suggested that the residue corresponding to D401 in *T. reesei* Cel6A might act as the catalytic base in family 6 glycosyl hydrolases.[13,41,42] However, probing into the function of this residue in other family 6 enzymes by mutagenesis studies has led to contradictory results. The data initially obtained with CenA from *C. fimi* supported its role as the base,[41,42] while recent experiments with *T. fusca* E2 reveal a dramatic decrease in substrate binding.[43] In the structure of *T. reesei* Cel6A, D401 has numerous hydrogen bond acceptor interactions to the nearby side chains of R353, Y306, K395 and the main chain of residue 369 that would ensure a low pK_a for this carboxylate. Furthermore, in the structures that we have determined to date, the carboxylate group of D401 is seen to interact with the O3 hydroxyl, at the edge of the glucosyl unit in the −1 site,[18] Figure 1. Loss of this interaction may account for the decreased binding observed in the related *T. fusca* E2 enzyme.[43] The data obtained in ref 43 and the structural data discussed above thus argue against the role of D401 as a base. The structural data indicate that D175, together with S181, participates in the coordination of the two water molecules that are most closely positioned to attack the anomeric carbon, Figure 1. The crystallographic structures cannot resolve their charge states, but one water, coordinated by the S181 side chain and the D401 backbone carbonyl oxygen, is only 3.3 Å from the anomeric carbon. The molecular dynamics simulation of the carbocationic intermediate suggests that this water is stably coordinated and is the most probable candidate for the catalytic water. This remains connected to D175 via the second water molecule observed in the crystal structure of the Y169F/$(Glc)_2$-*S*-$(Glc)_2$ complex. The candidate catalytic water is 6.0 Å from the carboxylate group of D401, and this residue undergoes no conformational changes in any of our crystallographic studies. It seems possible that, rather than removing the catalytic base, mutating the residue equivalent to D401 in other family 6 enzymes introduces a charge imbalance that may destabilize an oxycarbenium-ion-like transition state. Its removal would leave two positively charged side chains, R353 and K395, without compensating acidic groups close to the −1 site.

Proton Transfer from the Nucleophilic Water. Because there is very little bond formation to the nucleophilic water in the transition state of *T. reesei* Cel6A, there is little need for efficient base catalysis. One possibility, suggested by the experimental structures, is that a proton is transferred from the nucleophilic water, via the second water, to D175 in a Grotthus-type mechanism. To investigate this, we measured the solvent isotope effect on k_{cat} for the hydrolysis of the poor substrate, cellotriose. With such a poor substrate, noncovalent events such as product release are unlikely to limit k_{cat}, and the effect is probably intrinsic. The value obtained, 1.16 ± 0.14, was surprisingly small considering literature precedents; one would expect direct contributions both from the proton transfer to the poor leaving group and from the nucleophilic water. In model systems, general acid catalysis of acetal hydrolysis is associated with values of k_{H2O}/k_{D2O} of 1.5−2.5.[52−54] Solvent isotope effects (k_{H2O}/k_{D2O}) on nonenzymic reactions, in which water is a nucleophile and the leaving group does not require protonation, are in the region 1.2−2.1,[55,56] increasing with the nucleophilic involvement of water. A proton inventory on glucoamylase-catalyzed hydrolysis of a substrate with a good leaving group suggested that the effect of 1.8 arose solely from the proton being transferred from the nucleophilic water to the catalytic base.[57] The contributions to the solvent kinetic isotope effect therefore cannot be just changes in fractionation factors of the acid catalyst and nucleophilic water, which would give an effect of 2−3. A large inverse contribution must also be involved. This could, for example, be the rupture of a short, tight hydrogen bond in a preequilibrium step. Such hydrogen bonds are characterized by low fractionation factors; a value of 0.4 has been reported for the hydrogen bond between the catalytic aspartate and protonated histidine in chymotrypsinogen.[58] A short hydrogen bond exists between D221 and D175 in the unliganded enzyme (D221 OD2, D175 OD1 separation 2.7 Å) and persists in the Y169F/$(Glc)_2$-*S*-$(Glc)_2$ complex (D221 OD2, D175 OD1 separation 2.5 Å), which is our closest analogue of the ES complex with cellotetraose.[18] This hydrogen bond must be broken before D221 can act as an acid, and, if rapid and reversible, its breaking will make a large inverse contribution to $^{D2O}(V)$. A solvent isotope effect close to unity is thus anticipated for the active-site architecture revealed by crystallography.

Conclusions

Our model for the roles of the active-site residues D221 and D175 of the *T.r.* Cel6A is the following: (1) D221 acts as the catalytic acid, and (2) D175 acts to stabilize a uniquely electron-deficient transition state through electrostatic interactions. It also modulates the pK_a of D221 and may act as a proton acceptor through a water chain. The degree of proton transfer at the transition state, however, is very slight.

Acknowledgment. At VTT, we are grateful to Arja Lappalainen, Tarmo Pellikka, and Susanna Virtanen for the help in

(50) Bakthavachalam, V.; Lin, L. G.; Cherian, X. M.; Czarnik, A. W. *Carbohydr. Res.* **1987**, *170*, 124−35.
(51) Cherian, X. M.; Van Arman, S. A.; Czarnik, A. W. *J. Am. Chem. Soc.* **1988**, *110*, 6566−6568.
(52) Capon, B.; Smith, M. C.; Anderson, E.; Dahm, R. H.; Sankey, G. H. *J. Chem. Soc. B*, **1969**, 1038−1047.
(53) Anderson, E.; Fife, T. H. *J. Am. Chem. Soc.* **1969**, *91*, 7163−7166.
(54) Fife, T. H.; Brod, L. H. *J. Am. Chem. Soc.* **1970**, *92*, 1681−1684.
(55) Lee, I.; Koh, J.; Park, Y. S.; Lee, H. W. *J. Chem. Soc., Perkin Trans.* **1993**, *2*, 1575−1582.
(56) Zhu, J.; Bennet, A. J. *J. Am. Chem. Soc.* **1998**, *120*, 3887−3893.
(57) Huang, X.; Surry, C.; Hiebert, T.; Bennet, A. J. *J. Am. Chem. Soc.* **1995**, *117*, 10614−10621.
(58) Markley, J. L.; Westler, W. M. *Biochemistry* **1996**, *35*, 11092−7.
(59) Harris, M.; Jones, T. A. J. *Acta Crystallogr.* **2001**, *D57*, 1201−1203.
(60) Nicholls, A.; Sharp, K.; Honig, B. *Proteins: Struct., Funct., Genet.* **1991**, *11*, 281.

protein purification, Anne Valkeajärvi for help in HPLC analysis, and Tuula Kuurila, Riitta Suihkonen, and Ulla Lahtinen for skillful technical assistance. Röhm Enzyme Finland is thanked for the fungal expression strains, and David Wilson is thanked for helpful comments on the manuscript. This work has been supported by grants from Nordisk Industrifond, the European Commission (Projects BIO2-CT94-3030 and BIO4-CT96-0580), the Academy of Finland, and the Swedish Natural Science Research Council, NFR (T.A.J.).

Supporting Information Available: Molecular biology protocols, details of the chemical syntheses, procedures for protein crystallization, and structure determination (PDF). This material is available free of charge via the Internet at http://pubs.acs.org.

JA012659Q